energies

Article

Method and a Device for Testing the Friction Force in Precision Pairs of Injection Apparatus of the Self-Ignition Engines

Jan Monieta

Maritime University of Szczecin, Wały Chrobrego 1-2, 70-500 Szczecin, Poland; j.monieta@pm.szczecin.pl; Tel.: +48-91-48-09-415

Abstract: This article reviews the state of the knowledge and technology in the field of friction-loss measurements in internal combustion piston engines. The dependencies that describe the loss of energy in combustion engines and injection apparatus are presented. Currently, very little can be found in the literature on the study of frictional forces in injection apparatus, but mainly in the piston–cylinder group, so this work significantly fills that gap. The aim of this article is to construct a device and to develop a method for assessing the technical state of injector nozzles to minimize friction losses in internal combustion engines at the stages of evaluation, design, production and operation. This article presents a stand for determining the maximum friction forces due to gravity loading by water-jet control. This article also presents test results on the maximum friction force between a needle and a body of injector nozzles in piston combustion engines on a designed and purpose-built stand outside of the combustion engine. Various designs and injector nozzles are made from various types of alloy steel for marine and automotive piston internal combustion engines fueled with distillation or residual fuels, and are tested. The research concerned conventional elements for the injection apparatus as well as electronically controlled subsystems. Precision pairs of injection equipment are selected for the tests: new ones are employed after the storage period and operated in natural conditions. The elements dismantled from the internal combustion engines are tested in the presence of fuel or calibration oil of similar properties. The maximum static frictional forces under the hydrostatic loading are measured, alongside the parameters for the dynamic movement of the nozzle needles from bodies of the injector nozzle as time, speed, acceleration and dynamic force. The influence of the angular position of the needle in relation to the bodies of the precision pairs conventional internal combustion engines, the diametral clearance between the nozzle body and needle, and the surface conditions on the values of the maximum friction force are also presented. Errors in shape and position result in the uniqueness of the friction force at the mutual angular position of the needle in relation to the nozzle body, and the decrease in diametral clearance and deterioration of the surface state increase the friction losses. A model was elaborated of the influence of various factors on the value of the maximum friction force.

Keywords: internal combustion engines; injection apparatus; precision pairs; friction force; energy losses; measurements

check for updates

Citation: Monieta, J. Method and a Device for Testing the Friction Force in Precision Pairs of Injection Apparatus of the Self-Ignition Engines. *Energies* **2022**, *15*, 6898. https://doi.org/10.3390/en15196898

Academic Editors: Enhua Wang and Baofeng Yao

Received: 23 July 2022
Accepted: 15 September 2022
Published: 21 September 2022

1. Introduction

The internal combustion engines of marine vessels consume a large amount of fuel, which is the highest cost (up to 50%) in ship operations [1]. The problems of climate change and the reduction in fossil fuels has necessitated research focused on improving the efficiency of internal combustion engines. The minimization of friction losses in combustion engines is a primary goal, in order to improve performance and to comply with increasingly stringent legislative requirements. When operating means of transport powered by an internal combustion engine, it is advisable to use one with as low a fuel consumption as possible and to reduce the emission of toxic exhaust components. Global environmental awareness has become important, and has placed significant new technical requirements on means of transport including the improvement of engine efficiency, which is directly related to the production of carbon dioxide and the emission of harmful exhaust components [2]. The striving for improved fuel economy and the rigorous emissions control of low-speed marine diesel engines have made technologies for reducing engine friction a problem for designers and a concern for manufacturers [3]. The estimation of friction losses is recommended at the stage of valuation and design. The estimation of friction losses in engine component models requires necessary geometric and functional inputs [4]. To enhance the efficiency of combustion engines, different approaches have been taken, including improvements in advanced combustion processes, reducing the component sizes and the introduction of electrification and heat-recovery systems.

One method is to minimize the energy losses due to friction at the design stage, and manufacture and operate the internal combustion engine in the friction nodes. The injection subsystem, including the injection apparatus, is one of the most unreliable subsystems of compression–ignition internal combustion engines [5]. Simultaneously, the injector apparatus determines the course of the working processes, the efficiency and the ecological values of engines. These elements have received little attention especially in terms of friction losses, apart from the works of the author and co-authors [6–8].

The present article mainly focuses on the injector nozzles of the marine compression-ignition engines, but research was also carried out for car engines and other precision pairs. The increase in the frictional power is an important measure of the wear processes that take place in the tribological nodes, and it is a factor that determines the efficiency of the machines [9].

The main aim of this article is to present a method and an actual device for measuring the course and the value of the friction force in the precision pairs of the injection apparatus, used in the presence of lubricants. An auxiliary goal is to determine the share of the mechanical losses in the injection equipment of marine internal combustion engines.

2. Friction Power Losses

2.1. Friction Power Losses in Piston Internal Combustion Engines

The energy performance of an combustion engine depends on the quality and the properties of the fuel used to fueled with it. The individual components of the energy conversion process that are realized in a combustion engine can be represented in the form of an engine power balance. The general equation for the balance in a four-stroke medium-speed marine engine can be written as:

$$E = E_e + E_{co} + E_o + E_{in} + E_m + E_h + E_r \tag{1}$$

where E denotes the energy stream supplied to the engine in the fuel, E_e signifies the useful energy stream, E_{co} is the cooling losses (i.e., in the pistons, cylinder liners and heads, injectors, turbochargers, charge air, etc.), E_o is the outlet losses, E_{in} is the energy stream for the incomplete combustion losses in the self-ignition engines, E_m is the energy flux lost to the mechanical losses, E_h is the stream of energy lost to the environment through heat exchange, and E_r represents the flux of the rest of the losses and the heat-balance error.

The mechanical losses of the combustion engine power N_m can be written:

$$N_m = N_f + N_{ch} + N_p + N_o \tag{2}$$

where N_f is the frictional power, N_{ch} is the power for the exchange process, N_p is the power to drive the auxiliary mechanisms and N_o is other losses.

The characteristics of the lubrication systems and the quantification of the friction losses are vitally important factors for the design of durable combustion engines with improved fuel economy, as shown in [10]. An article by Karczewski [11] presents the methodology and the measurement results for the internal resistance of a self-ignition engine. The resistance to the movement introduced by individual functional systems was determined, such as the piston crank, the exchanges of the working-medium system, the fuel-feed system, the cooling, the lubrication, the automatic steering and the control system directly related to the engine operation, as well as the percentage share of related power losses for the drive of individual systems and self-ignition engine units. The frictional power losses (N_f) are approximately 70% of the above losses and this constitutes the largest part of the mechanical losses [11].

Friction occurs in all the kinematic pairs of the associated elements.

The crosshead slipper–guide pair and the piston skirt–liner pairs are two important friction systems in low-speed marine self-ignition engines [3]. The consumption of friction power by the crosshead slipper, however, is larger than that of the piston skirt [3].

Compression ignition engines lose their energy to friction by around 4–15% of the total input energy [12]. Most of these friction losses result from the piston–cylinder system which contributes around 20 to 55% of the mechanical friction losses via these numbers, also include the power loss from the piston rings. For this reason, modernized materials or processes for the in-cylinder component of the marine diesel engines have been widely studied for improving the friction efficiency [13].

Ruddy et al. reported that approximately 5–7% of the total produced power is lost via the mechanical friction, of which 44% is from the piston assembly, 13% is the crankshaft, 10% is the large-end big-end bearing 10%, 6% is the valve-train mechanism and 5% is the oil-churning and oil-flow losses, while the 22% that remains has not been assigned [14]. Livanos et al. [15] investigated the friction components of the compression rings, the oil-control rings, the piston skirt, and the gudgeon pin of the engine piston assembly.

The portion of the frictional losses from the different elements of a large two-stroke marine diesel engine is not well-known [16]. The engine and the car-engine sub-assemblies' friction losses were investigated over a full speed and load range, for more than 120 engine-operation points at different engine media supplied temperatures, ranging from 70 to 110 °C [17]. For the investigated self-ignition engine, a friction-reduction potential of up to 21% was determined, when changing the engine and the parts load operating conditions. At low crankshaft speeds and high load operations, the friction loss reduction potential is decreased considerably and is below 8%, which according to Knauder et al. were caused by indication of mixed lubrication regimes at the piston–cylinder group and valve train [17].

The greatest techniques for reducing the friction of tribological components in reciprocating engines are being realized currently through advanced low-viscosity engine oils, low-friction coatings, and surface texturing [10,18].

2.2. Friction Power Losses in Injection Apparatus

Currently, the literature mainly focuses on research on the friction losses in the piston ring–cylinder liner pairs, while other losses are marginalized [3,10,12–14]. The power losses due to friction in the fuel system, including the filters, the feed pump, the supply lines, the injection pumps, the injection lines and injectors are significant. Of the auxiliary systems of combustion engines, fuel injection is the one with the highest percentage of total losses, totaling 6.6% [19]. The results of the experimental test carried out on a single-cylinder self-ignition engine showed that the energy losses of the fuel injection subsystem are equal to 0.61% of the chemical energy of the injected fuel [19]. Losses for overcoming friction forces in the injection apparatus have an impact on the friction losses in other functional systems, such as the fuselage and the piston-crank system. The power losses in the injector nozzles are shown in Figure 1. A sum of the losses for overcoming the external and internal interactions can be determined, which is described in relation to N_{in}:

$$N_{in} = N_{ns} + N_{ic} + N_{cs} + N_{sp} + N_{cs} + N_s + N_{ih} + N_{cp} + N_{co} \quad (3)$$

where N_{ns} is the power lost to overcome the spring-tension force, N_{ic} is the power lost in the fuel inflow channels, N_{cs} is the power lost in the choking space, N_i is the power lost to overcome inertia forces in reciprocating motion, N_{sp} is the power lost to friction in the guiding part of nozzle needle, N_{cs} is the power lost in the sealing cone, N_s is the power lost in the suck volume, N_{ih} is the power lost in the spraying holes, N_{cp} is the power lost to overcome counterpressure in the combustion chamber and N_{co} is the power lost to the cooling of the injector nozzle.

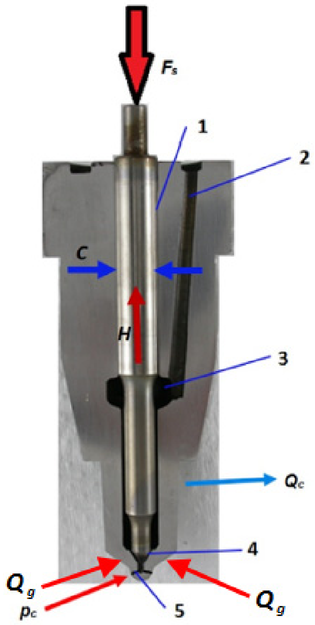

Figure 1. Interactions on the injector nozzle and the positions of frictional power losses: 1—guide part between the nozzle body and the injector needle, 2—inlet passage, 3—throttling space, 4—sealing cone and 5—atomization hole. In addition, C is the gripping force caused by the deformation of the injector nozzle, F_s is the spring tension force, H is the hydrodynamic pressure force, Q_c is the heat loss for injector-nozzle cooling, Q_g is the thermal load with combustion gases, and p_c is the counterpressure in the combustion chamber.

In a nozzle needle–nozzle body pair, the load mainly acts along the axis of the needle. The side thrusts may occur as a result of the shape and the position errors, the elastic deformations and the loads caused by the fuel pressure on the surfaces in the gaps between the body and the nozzle needle [20–22]. However, the reduction in friction in the gaseous-fuel-injection apparatus is much more important. In the work by Baratta et al. [23], the injector-needle design was elaborated with the aim of reducing the injector's internal friction, which causes injector wear due to a lack of any lubrication effects, as is the case to liquid-fuel injectors.

The friction surfaces in the precision pairs of the injection apparatus are lubricated with fuel, essentially by leakage. The force of the friction in a nozzle needle–guide pair depends on the fuel properties, the pressures and the coefficient of friction; for a mixed friction situation this can be written as:

$$T = \eta c A f(x) \tag{4}$$

where A is the friction surface, c is the planning speed, $f(x)$ is the shape function and η is the fuel viscosity.

There is also a friction force that depends on the fuel properties, the planning speed, the mixed friction from pressures and the coefficient of friction [24]:

$$T = f(P, c, X_c) \tag{5}$$

where P is the load and X_c is the tribological properties of the medium.

If the nozzle elements do not change their position in relation to each other, there is a rest friction between them, or a moving friction when they are in relative motion [25].

The injector nozzles of marine internal combustion engines are operated in extremely unfavorable conditions under the influence of high fuel pressure and are subjected to thermal, mechanical and chemical loads [22,24,26]. As a result of these extortions under the influence of various external factors, there is intense friction, wear and damage, alongside changes in the design parameters of the injection apparatus, and a transition from a state of full ability to either an acceptable state or state of disability [27,28]. In the event of needle immobilization, the nozzles lose their tightness and additional fuel enters the cylinder, which will be combusted without enough oxygen. Next, deposits intensively form on the surfaces of the injector nozzle. If the needle is partially seized, the system is raised at a higher fuel pressure and a different speed.

Reducing the tightness of the contact between the sealing cones of the needle and the nozzle body causes an penetration of hot gases from the combustion chamber to the inside of the injector nozzle. As a result, the surfaces of the injector nozzle are heated and the needle seizes up due to the loss of lubrication; heat begins to build, deformations occur, and unwanted deposits are made. Strong heating due to friction acting against the walls of the nozzle causes a significant increase in the temperature of the fuel and a decrease in its viscosity of the fuel [29].

When the fuel flow during the injection is at pressures of up to 300 MPa, large velocity gradients are generated that induce wall friction and a strong heating [30]. In the injector nozzle, a fuel stream at a pressure of 450 MPa in the sac volume splits into two legs: one corresponds to a cooling down of the core flow, while the other involves a heating due to the wall friction [31].

Nozzle needle immobilization occurs when the friction force, T, between the body and the nozzle needle is greater than the force that causes its displacement, F_p (i.e., the spring tension or the hydrodynamic fuel pressure acting on the surface of the needle), namely:

$$T \geq F_p \tag{6}$$

A seizing is defined as an inhibition of the relative movement of the elements of the friction pair [32].

The technical state of the nozzles is determined by the values of the features, such as shown in [28]: geometrical dimensions, mutual clearances of cooperating elements, the surface state in tribological nodes, etc.

The literature [8] and current patents [33,34] show that an important aim is to minimize the friction losses in internal combustion engines, which results in lower fuel consumption (Holmberg et al. [35] and Zabelin [36]).

Monieta and Kasyk [8] presented a simulation model for the injector-nozzle structure of a marine self-ignition engine with an optimization of the design to reduce fuel-flow losses. One of the design features of the injector nozzles, which influence the fuel injection process, is the geometry of the nozzle holes.

Longwic et al. [37] wrote that the use of rapeseed fuel with a higher viscosity results in increased friction losses for the elements of the injection apparatus that move relation to each other (i.e., the piston–cylinder of injection pump, the unloading valve, the body and the injector needle). The authors also provide formulas for the resistance forces to motion and the friction coefficients in the elements of the injection sub-system.

Lopez et al. [38] provided a methodology for characterizing the pressure losses in the quasi-stationary common-rail injectors of the self-ignition engines that have been developed. The authors used the friction coefficients in their calculations.

The methods for testing the friction force in injector nozzles are not often undertaken [6,8,19,22], but some are described in [6,7].

3. Tests of Friction Force in Injectors of Combustion Engines

Theoretical and experimental tribological studies may concern the processes and the phenomena that occur during friction, wear and lubrication. In precision pairs of injection apparatus, a mixed friction also occurs, and the value of the friction force is influenced by the condition of the mating surfaces and the type and quality of fuels that are used [20,24].

These factors have a significant impact on the durability and reliability of elements of the injection apparatus and the other elements of internal combustion engines.

The literature [39] describes a method for calculating the frictional force of a body on an inclined plane. Dudziak et al. [40] presented the test stands for the measurement of the force and the moment of friction of a sleeve–shaft couple. The sleeve was connected with shafts that were manufactured with radial error, cross-section deviations, and combinations of both. Experimental investigations were performed to determine the influence of the form deviations and the angular positions of the shaft on the value of the axial friction force (during the shaft sliding) and the moment of friction (during the shaft rotation).

So far, during accepted tests for injector nozzles, it has only been checked whether the friction force between the body and the needle was smaller than the force that results from the component of the gravity or not, as described in [41]. Knauder et al. [17] reported that the friction losses of the fuel pump were not of much interest, and therefore have not been studied.

The patent descriptions [33,34] only provide a method for reducing the friction force in the injector nozzles. From another patent document [42], there is known to be a method for determining the opening pressure of an injector nozzle and a system for implementing this method. This informs us that the friction generated in the process will constitute a disturbance variable for determining this pressure, which reduces the accuracy of the measurement. The device according to the invention provided by the patent document [43] is intended for measuring the load force and the friction force in a tribological system. The device comprises a set of two sensor deformations that act in two opposite directions. Each sensor deforms in one direction under the lifting force and counteracts under the frictional force measured by two consecutive pairs of strain gauges located on opposite sides of the bundles.

4. Test Method

4.1. Measurement Method

One method used to measure the friction force component involves the setting of a stationary sample in motion under the action of gravity. This allows the maximum force of the resting friction to be calculated. It is also possible to measure the amount of time needed for the sample to move under the influence of the weight that is needed to propel the sample.

The aim of such an invention is to construct a device and to develop a method for assessing the technical state of its injector nozzles at the production and the maintenance stage, outside of the internal combustion engine. So far, during the acceptance tests of the injector nozzles, it is typically only checked whether the friction force between the body and the needle is smaller than the force that results from the force component of gravity or not, as was described by Piaseczny [41]. After the needle is seated in the nozzle body, it can be checked by lifting the needle one-third of its length, at an angle of 45°. If the needle falls on the seat without stopping under the action of its own weight, the technical state can be considered correct. In this way, the injector nozzles are assessed in two states (i.e., full ability or partial disability) without a quantitative measurement. The scatter of the results for the friction force between the nozzle body and the injector needle may be large, up to a state in which there is immobilization, which has significant effect on the engine performance [6].

The essence of this method is to verify that the nozzle needle traverses from rest to motion under the action of its own gravitational force, due to the nozzle body set at an angle of 45° with the needle pin facing downwards. An additional and a gradual gravity force is applied to the needle pin along the longitudinal axis of the injector nozzle until the needle is completely removed from the nozzle body.

The measurement of the friction force was performed after washing the injector nozzle with a mineral solvent and supplying a lubricant to the guide parts, which may be fuel or calibration oil used for testing the injector nozzles with the same properties. Calibration Shell oil was used in these tests.

The maximum friction force measurements are made with respect to the nozzle body in at least four positions of the needle, in 90° increments. Due to the shape and the position errors, there is a diversified distribution of the friction force alongside the position of the body in relation to the nozzle needle.

4.2. Measurement Stands

The essence of the test device solution consists of a structure designed and built in sections, which has a plane inclined at a 45° angle, attached to the base plate of the stand by means of screws. It has a limiter located on the vee block, which fixes to the tested injector nozzle (Figure 2).

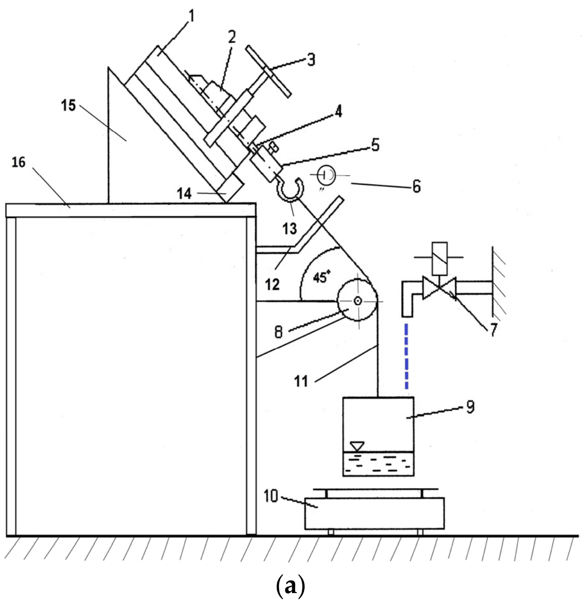

Figure 2. Diagram of the test stand for measuring the friction force of the needle in the nozzle body before extending the needle (**a**) and after removing the needle from the nozzle body (**b**): 1—steel vee block, 2—tested injector nozzle, 3—mounting screw, 4—nozzle needle, 5—holder, 6—photocell controlling valve 7, 7—water shut-off solenoid valve, 8—roller, 9—container for accumulated water, 10—electronic laboratory scales, 11—line, 12—extension limiter of nozzle needle, 13—hook, 14—limiter of vee block, 15—inclined plane 16—main plate of stand.

The device is equipped with a specially designed and manufactured holder that consists of a metal body in the shape of a cylinder (marked as 5) with an axially drilled cylindrical channel with a diameter that ensures a free insertion of the pin of the nozzle needle and mounting with a screw; the hook (13) is free to rotate around the longitudinal axis (Figure 3).

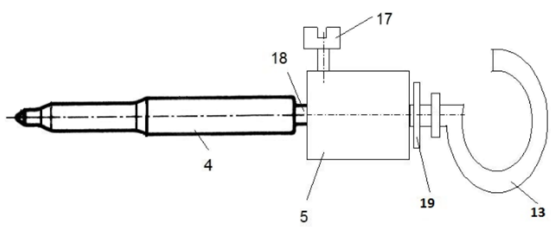

Figure 3. Holder mounted onto the pin of the nozzle needle: 4—nozzle needle, 5—holder body, 13—hook, 17—needle fixing screw of nozzle needle, 18—nozzle needle pin and 19—spacer ring.

The value of the maximum friction force between the nozzle body and needle is influenced by the state of the mating surfaces and their mutual location, contamination, etc. Therefore, before any measurements are made, all the tested injector nozzles are washed with gasoline or with another mineral solvent, and then they are dried and blown with compressed air.

The nozzle body (2) is attached to the steel vee block (1), with the bow (3), so that the protruding pin (18) of the needle (4) is at the bottom of the vee block. The vee block is attached to the plane (15) with bolts, and the askew plane is inclined at a 45° angle to the station base plate (16) near its edge and it is secured by the stop (14) against any movement. The tested injector nozzle is set at an angle of 45°, which is dictated by a method of checking the free protrusion of the needle during the verification of the nozzles at the stage of production and operation. The device is equipped with a holder (5) of a nozzle needle, to which a rotating hook (13) with a spacer ring (19) is attached to a line (11) suspended over a roller (8) and it is connected on the other side with a vessel (9) filled with water from the solenoid valve (7), which is located above the vessel. The line-guiding roller is attached at a suitable distance, which ensures a line-inclination angle of 45°, and is parallel to the longitudinal axis of the injector nozzle.

A holder (5) is screwed onto the pin (18) of the nozzle needle (4), which is connected by a rotating hook (13) to the line along the axis of the needle, and on the other side, the line is slung over the roller (8) and it is connected to the empty vessel (9). The pin of nozzle needle (18) slides into the axial bore of the holder (5) (Figure 3) and it is fixed with a screw (17) before moving. The guide part of the needle should slide completely out of the injector body until it is beyond the face of the nozzle body (Figure 2b).

The gradual increase in the friction-force component, from the value 0 to the maximum value (Figure 2), is performed by means of a small and regulated stream of water that is supplied through the valve (7) and, in the case of a very low value, it is also possible to dose via a syringe into a suspended small vessel (9). After the needle is completely extended beyond the front surface of the nozzle body and the holder (5) and rests against the limiter (6), the water supply to the vessel (9) is automatically switched off by control with the photocell (6). The vessel with water must be weighed together with the line and holder at the scales (10) with a digital readout, which is an additional mass, and the nozzle needle must also be weighed. The weight of the nozzle needle m_n, and the additional weights determined in this way, enables a determination of the force component from gravity and the maximum friction force (Figures 4 and 5).

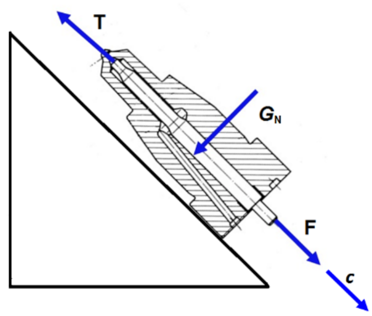

Figure 4. Forces acting on the needle in the cross-section of the injector nozzle, in which c—needle movement speed, F—force acting on the needle, G_N—gravity force component perpendicular to the inclined plane and T—static friction force.

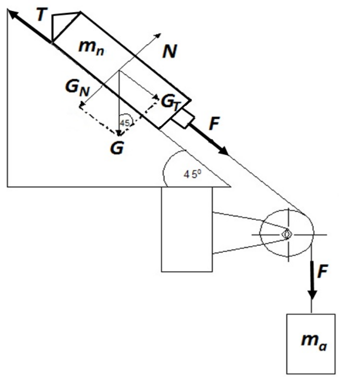

Figure 5. Model of the distribution of the forces the act on the nozzle needle, in which G_T—gravity force component parallel to the inclined plane, m_a—additional mass, m_n—mass of the needle and N—pressure force perpendicular to the surface.

Based on Figure 5, a formula can be written for all the forces that act on the nozzle needle:

$$G_a + G_T - T = 0 \tag{7}$$

By transforming this relationship, the maximum force of static friction is determined:

$$T_{max} = max(T) = max(F + G_T)\ [\mathrm{N}] \tag{8}$$

As the load from the inlet water jet gradually increases, the force acting on the needle in the injector body increases. This enhances both the contact force N and the friction force. The static friction occurs if the needle is at rest; only when the load is sufficiently does the needle begin to move. This maximum force due to static friction, for which the nozzle needle is still at rest, is the so-called limit-friction force. Thus, the force of static friction T_s can vary from zero to a certain maximum value T_{smax}, so that:

$$0 \leq T_s \leq T_{smax} \tag{9}$$

The value of the static friction force is proportional to the value of the pressure force N of the needle on the injector-nozzle body:

$$T_{smax} = \mu_s N \tag{10}$$

where μ_s is the coefficient of the static friction.

The force required to extend the needle from the nozzle body F is equal to the additional weight G_a on the needle pin with the substitution of the additional mass m_a and the acceleration of gravity g into Formula (11). This causes the needle to move with the force:

$$F = m_a\, g \tag{11}$$

The component parallel to the inclined plane is equal to the product of the mass of the nozzle needle m_n and the acceleration of gravity g, so that $G_T = m_n g$ and the sine of the inclination angle is equal to $\alpha = 45°$. Therefore, the final formula determined for the static friction force used in the calculations is given by:

$$T_s = m_a g + m_n g \sin\alpha\ [\mathrm{kg \cdot m/s^2 = N}] \tag{12}$$

In the case when the needle comes out by itself from the nozzle body under its own weight, the additional weight is not needed, i.e., $F = m_a g = 0$, and the formula for the friction force will simplify to the following form:

$$T_s = m_n \cdot g \cdot \sin\alpha \tag{13}$$

The frictional force that acts on the nozzle needle, while in motion, is called the kinetic friction or the dynamic friction [44]. The value of the dynamic frictional force depends on the value of the pressure force (for the needle on the leading part of the injector body), which is marked as N. This relationship is directly proportional to the friction coefficient of the motion, $\mu_d(c)$. This is not a constant, but depends on the relative velocity of the rubbing bodies. Therefore the dynamic friction also changes with speed, so that:

$$T_d = \mu_d(c)N \tag{14}$$

where T_d denotes the dynamic friction force value and $\mu_d(c)$ is the motion-friction coefficient as a function of speed.

The research used geometric methods to determine these dimensions, as well as contact and non-contact devices from reputable companies for measurements, including micrometers, bore gauges, microscopes and profilometers [28]. The geometry of the tested objects was measured and analyzed using, among others, the WYKO NT1100 optical profilometer. Measurements of the shape and profile were made on a specialized instrument Hommel Roundscan 535. In addition to the measurements of typical geometrical deviations such as roundness, straightness and conicity, this instrument also enables the measurement of surface roughness.

Next, the course of the friction force is determined from the extension time and the course of the speed of the needle extending from the nozzle body. Here, too, significant variety in the time values was observed. Thus, apart from the vibrations of the elements, there are also oscillations in the value of the frictional force. The displacement of the injector needle was processed by the DT10, an eddy-current sensor that uses a designed and built holder (Figure 6). The displacement of the nozzle needle signals an acquisition and the analysis system was applied with analog-to-digital processing and data recording, using the measurement circuit described in [5]. After differentiating the displacement twice over time, the acceleration course of the advancing nozzle needle movement was determined, which enables us to calculate of the dynamic friction force T_d, i.e.:

$$T_d = m_n a \tag{15}$$

where $a = dh^2/d\tau^2$ is the acceleration of the injector needle. The needle acceleration during the extension from the injector body is calculated on the basis of movement along the axis of the nozzle needle. The needle lift was recorded by the measuring system outside of the combustion engine (Figure 6a), and displacements transverse to the nozzle needle axis recorded by the signals processing system and part of the stand (Figure 6b) were used to determine the beginning and end of the needle movement and the duration of the stroke from the nozzle body for the measured lengths. At higher values of the friction force, for other measuring stands, the time waveform of the dynamic friction force is directly recorded via $T_d = f(\tau)$ [6,7].

The average of the applied measurements in at least four planes, T_{maxi}, is taken as the final value of the maximum friction force:

$$T_{maxa} = \frac{1}{n}\sum_{i=1}^{i=n} T_{maxi} \tag{16}$$

where n denotes the number of planes in which the i-th value of the maximum friction force is measured.

The power, N_T, of the friction losses is calculated for the conditions of the internal combustion engine as the friction work is performed by the dynamic friction force $T_d = f(\tau)$ on the needle-stroke path, $h = f(\tau)$, during the τ needle lift in time of the fuel injection process, so that:

$$N_T = \frac{L_T}{\tau} = \frac{T_d h_{max}}{\tau} \tag{17}$$

where L_T represents friction work and h_{max} is the maximum nozzle needle stroke. In order to determine a frictional power that is comparable for positions outside of the engine, it is calculated on the basis of the maximum stroke of the needle.

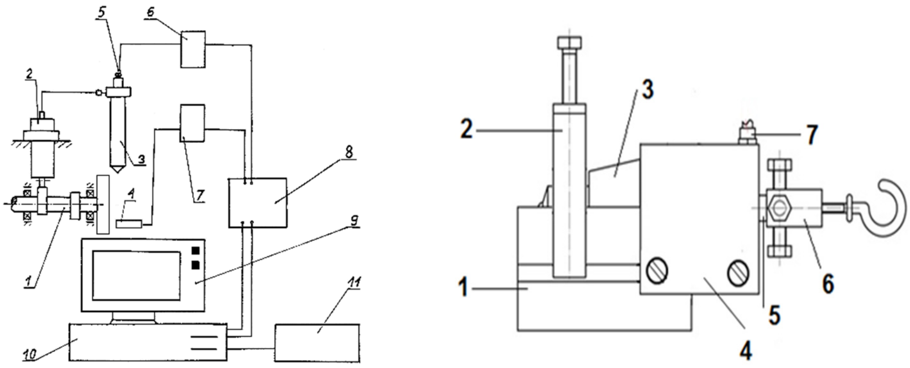

Figure 6. The measuring circuit for the acquisition and processing of nozzle needle-lift signals (**a**): 1—camshaft, 2—injection pump, 3—injector, 4—photo optical crankshaft position sensor, 5—eddy-current sensor of the lift of injection needle, 6—amplifier, 7—amplifier, 8—terminal connection, 9—monitor, 10—computer, 11—printer; the part of the stand of signal processing the position of the feeding of the injector-nozzle needle (**b**), in which 1—steel vee block, 2—clamp, 3—injector-nozzle body, 4—displacement sensor holder, 5—nozzle needle, 6—nozzle needle holder, and 7—eddy current displacement sensor.

The friction power can be used to calculate the friction efficiency, η_T, of the injection apparatus for one cylinder of the internal combustion engine, which is represented by the following formula:

$$\eta_T = \frac{N_T}{N_i} \tag{18}$$

where N_i indicates the power of one cylinder. For the tested injector nozzles, the friction efficiency ranged from 0 to 0.0322%. Losses to friction in injector nozzles constitute a small share in friction pairs to losses in dominant pairs of combustion engines.

The essence of the invention is a device for determining the friction force and the method of its determination. Here, it is proposed to determine this quantitatively, as one of the measurable significant features of the technical state of the injector nozzles of internal combustion engines.

4.3. Estimating Measurement Errors

The measurement errors are estimated to increase the reliability of the method. The systematic absolute root means square error of the static friction force, $\sigma(T_s)$, is calculated by differentiating over the individual variables that appear in Formula (12), according to the relationship:

$$\sigma(T_s) = \sqrt{\left[\frac{\partial T_s}{\partial m_a}\sigma(m_a)\right]^2 + \left[\frac{\partial T_s}{\partial m_n}\sigma(m_n)\right]^2 + \left[\frac{\partial T}{\partial g}\sigma(g)\right]^2 + \left[\frac{\partial T}{\partial \alpha}\sigma(\alpha)\right]^2} \tag{19}$$

The systematic relative error of the static frictional force, $\overline{\sigma}(T_s)$, can be calculated from the following expression:

$$\overline{\sigma}(T_s) = \frac{\sigma(T_s)}{T_s} \cdot 100\% \tag{20}$$

The values of the relative error of the maximum static friction force is dependent on the mean square absolute error and the value of the measured friction force; these results are equal to $\pm 0.1\%$. The small error values arise from the high accuracy of the additional weight measurements. The relative maximum error of the signal processing of the measurement circuit is calculated as follows:

$$(P_e) = 100\% \sqrt{\left(\frac{\Delta_{bs}}{x_{ts} - x_{bs}}\right)^2 + \left(\frac{\Delta_{bp}}{x_{tp} - x_{bp}}\right)^2 + \left(\frac{\Delta_{bd}}{AD}\right)^2} \tag{21}$$

where Δ_{bs} represents the limiting absolute error of the sensor, Δ_{bp} denotes the limiting permissible absolute error of the power supply, $x_{ts} - x_{bs}$ is the measuring range of the sensor, $x_{tp} - x_{bp}$ is the measuring range of the amplifier, Δ_{bd} is the absolute error of the analog-to-digital converter and AD is the number of all the bits of the analog-to-digital converter. The greatest contribution when estimating this error is made by the nonlinearity of the needle displacement sensor.

5. Sample Test Results

5.1. Results of Measurements of the Maximum Static Friction Force

The numerous measurements were made using the hydrostatic and hydrodynamic method and the device for measuring the friction force between the body and the nozzle needle tip of the injectors in the marine and the automotive combustion engines. Technical data of the most frequently tested injector nozzles are presented in Table 1. An example of determining the static frictional force, according to Formulas (12) and (13), with the required additional mass applied to the pin and with an unnecessary additional weight, is presented in Table 2.

Table 1. Technical data of the tested injector nozzles.

Engine Type	AL20/24D	L16/24
Number of spray holes	7, 9	8
Spray-hole diameter [mm]	0.23; 0.25	0.29
Spray angle [°]	159	145
Needle lift [mm]	0.50	0.40
Needle sealing-cone angle [mm]	7, 8	6
Needle length without pin [mm]	39.3	75.7
License	Sulzer	MAN B&W

Table 2. Data for calculating T_{smax} from the measured components of the operated injector nozzles of an AL20 engine.

m_a kg	m_n kg	G_a N	G_T N	T_{smax} N	T_{smaxa} N
0.2068	0.02522	2.028	0.1748	2.203	2.097
0.2408	0.02512	2.361	0.1742	2.536	
0.1638	0.02512	1.606	0.1742	1.780	
0.1728	0.02512	1.694	0.1742	1.869	
0	0.02670	0	0.1852	0.1852	0.1852
0	0.02670	0	0.1852	0.1852	
0	0.02670	0	0.1852	0.1852	
0	0.02670	0	0.1852	0.1852	

The tests show that the value of the maximum friction force changes with the angular position of the nozzle needle, with respect to the nozzle body, for all the elaborated stands, as a result of significant errors in roundness and cylindricity as well as impurities, which make the repeatability of measurements difficult. Figure 7 displays a radar graph of the maximum friction force, which depends on the angle of rotation of the needle relative to the body of operated injector nozzle of the AL20/24 engine, in the presence of lubrication with calibration oil.

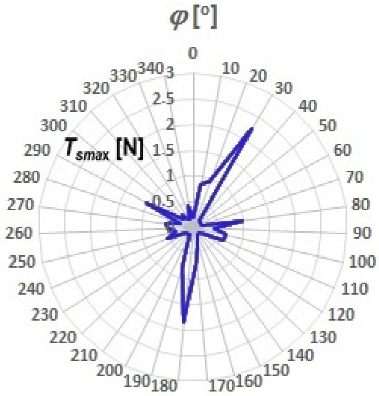

Figure 7. Radar graph showing the maximum value of the static friction force T_{smax} at different needle positions φ in relation to the one operated nozzle body.

The multi-hole injector nozzles were investigated mainly of marine reciprocating internal combustion engines, new and operated on seagoing vessels or cars. The investigated injector nozzles came from direct-injection self-ignition piston engines. They were usually in-line, non-reversible supercharged four-stroke engines and were equipped with turbochargers. Internal combustion engines were fueled with residual fuels, except during starting and stopping and when staying in certain ports.

The influence of the needle-position angle in relation to the injector body on the value of the maximum static friction force is significant.

Figure 8 shows the results of the exemplary measured maximum static frictional forces for the smaller values of the operated injector nozzles. Figure 8 displays a large variation in the average values of four measurements of the maximum frictional forces for various operated injector nozzles.

These values of the maximum frictional forces are determined by arithmetic means in at least four planes [6,7]. The progress of the developed method and device for measuring the friction force and the method of calculating friction losses is to propose implementation at the design, production and operation stage [8,41].

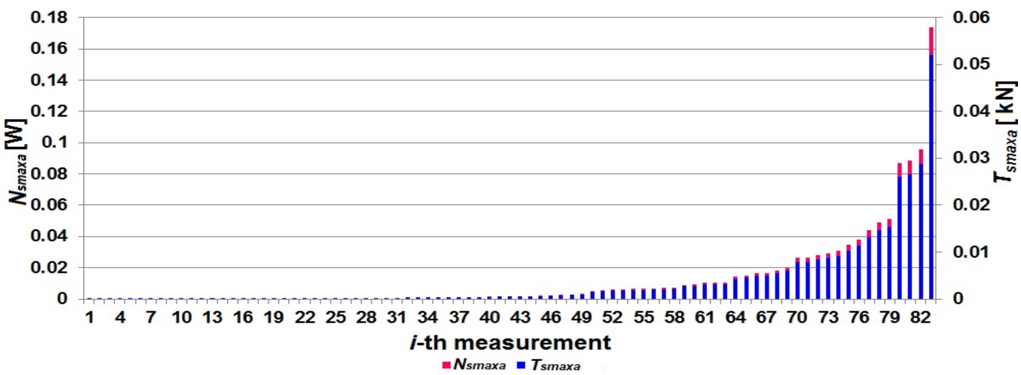

Figure 8. Systematized (in ascending order) for values of the measured average maximum static frictional forces T_{smaxa} and the values of the calculated frictional power, N_{smaxa}, of different injector nozzles of L16/24 marine engines.

5.2. Results of Measurements of Dynamic Static Friction Force

The research has shown that not only is the value of the maximum friction force important, but also the dynamics of the needle's movement. Some nozzle needles came out from the nozzle body due to the gravity component, but after a long time, which prompted the nozzle needle-protrusion-time measurements.

Figure 9a shows the registration of the shape of the nozzle needle s while extending the operated nozzle in the time domain τ from the operated injector-nozzle body of the AL20/24 marine engine. It is possible to calculate the average speed of the needle from the nozzle body c_a by dividing the length of the needle by the travel time, or for elementary increments. Figure 9b shows the values of the calculated average speed of the needle from the operated nozzle body c_a of AL20/24 marine engines in four planes, every 90°. These waveforms are significantly different for individual nozzles and for their measurement planes [6,7].

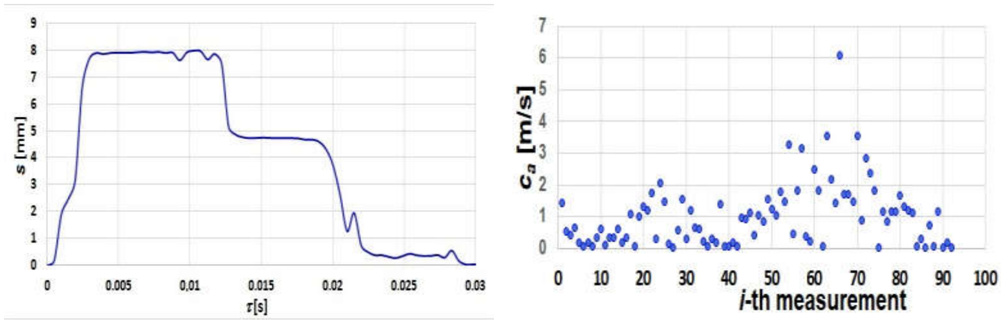

(**a**) (**b**)

Figure 9. Registration of the shape of the nozzle needle lift, s, at time τ, while extending from the nozzle body perpendicularly to the longitudinal axis (**a**) and the calculated average values of the speed of the needle extension from the nozzle bodies c_a (**b**).

5.3. Influence of Various Factors on the Values of the Maximum Friction Force

Among the causes of surface changes that affect the increased value of the frictional force, the dominant ones are the diametral clearance between the nozzle needle and the nozzle body, the type of fuel (i.e., distillation or residual), the quality of the fuel, deposit formations, condition of mating surfaces, etc. [6,7]. Residual fuels have an increased viscosity than distillate fuels and a high sulfur content [22,24].

From this and previous research by the author [6–8], it can be seen that the maximum frictional force is dependent on the important factors defined by this formula:

$$T_{max} = f(\varphi, m_a, G_T, c, \omega, \tau, l_t, m_t, D_c, D_f, S_r, S_d, F_q, W_{ib}, W_{in}.n) \tag{22}$$

where φ is the angle between the mutual position of the body and the nozzle needle, ω—angular speed, τ—time of movement of injector needle, l_t—length of the needle in the nozzle body, D_c is the diametral clearance, D_f is the deformation of the nozzle body and needle, S_r is the surface roughness, S_d—shape and position deviations of needle guide parts in the nozzle body, F_q is the fuel type and quality, W_{ib} is the wear of injector body, W_{in} is the wear of nozzle needle and n is the number of repetitions of measurements for each injector nozzle.

Figure 10a shows a field-of-view microscope image of an exemplary surface of the worn guide part of the nozzle needle of L16/24 marine engines. The image shows traces of processing during the production, abrasive wear, deposits formation from the fuel, corrosion, oxidation, etc. Figure 10b,c provide the guide parts of the nozzle needles, while the results of the maximum frictional forces are presented in Table 2. The state of the nozzle needle surface with a higher frictional force value (Figure 10b) is worse (i.e., more covered with deposits) compared to the nozzle needle with a lower friction force value (Figure 10c). The difference in the surface states was determined by an image-color analysis and a weighting of the deposit masses. The amount and quality of the resulting deposits on injector nozzles was determined by means of a global analysis of the blackening degree of gray images and the share of basic (red, green, blue) colors.

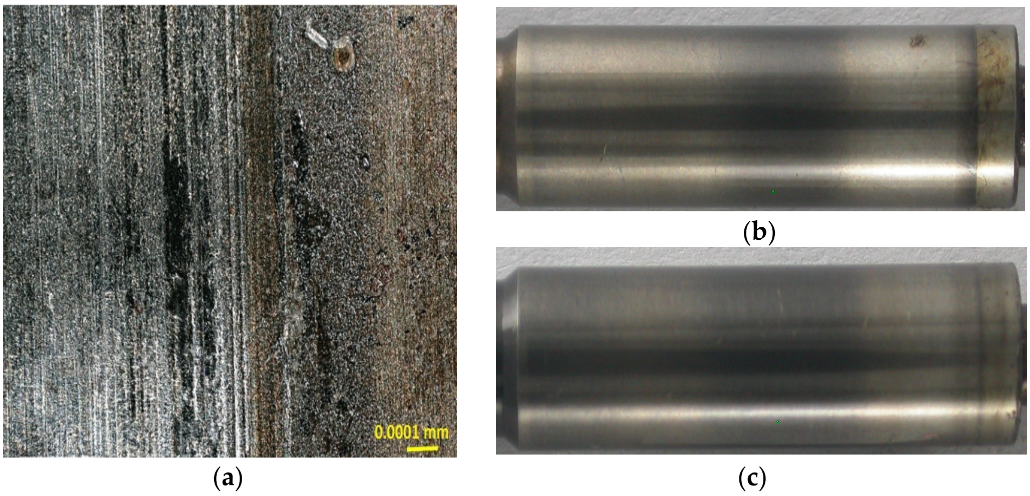

Figure 10. Surface state of an exemplary worn nozzle needle (**a**) at magnification of 300× and (**b**,**c**) the surface conditions of the nozzle needles at magnification of 5× for the friction forces presented in Table 1.

Additionally, in some cases, adhesive wear was also found. The identification of the types of wear was dealt with as presented in separate works [6,7,28].

The results of the surface roughness measurement of an exemplary nozzle needle of the L16/24 marine engine are shown in Figure 11a. The highest values were reached for the surface-inclination coefficient (kurtosis) and the average wavelength in Figure 11a. The influence of the diametral clearance on the values of the maximum friction force is presented in the histogram (Figure 11b). The figure shows that, in general, the static maximum frictional force is greater with a small clearance.

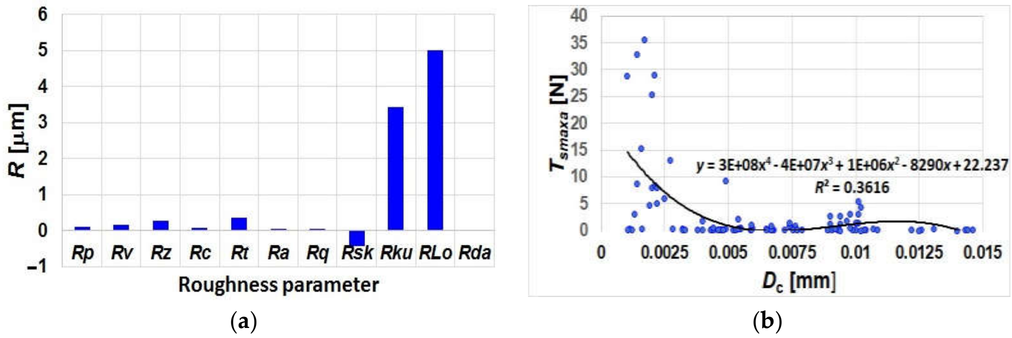

Figure 11. Plots showing the influence of the surface-roughness measurement of an exemplary nozzle needle (**a**) and influence of the diametral clearance, D_c, on the values of the maximum static friction force (**b**), in which R_p—maximum profile peak height, R_v—maximum profile valley depth, R_z—maximum height, R_c—mean height, R_t—maximum height of profile peak, R_a—arithmetic average, R_q—root mean square, R_{sk}—skewness, R_{ku}—kurtosis, R_{Lo}—average wavelength and R_{da}—average slope of the profile.

The geometrical structure of the surface of the friction pairs is a set of all real surface irregularities (deviations in shape, waviness, roughness), that significantly affect the value of the friction force. An advance in comparison with the newest and most modern similar research [18,19] is the understanding of the phenomena of friction, lubricants, wear and mechanical losses of combustion engines, especially in the injection subsystem [5,8,28]. This can be achieved by optimizing the structural design, including materials and surface conditions, by reducing the coefficient of friction and increasing wear resistance [7,13,18,28]. The beneficial effects of this method include the global measurement of the parameters, which is the maximum friction force between the body and the needle of the injector nozzle.

This method is an innovative, non-destructive diagnostic technique for characterization of mechanical losses in internal combustion engines with the use of symptoms expressed in numerical form. The article combines an innovative design with signal processing [5] and calculation of frictional power losses [8].

6. Conclusions

The essence of this invention is to build a device and develop a method for determining the friction force in precision pairs of injection apparatus of combustion engines.

The main advantage achieved by the method presented here is the possibility of quantifying the friction force, since it is one of the significant and measurable features for the technical state of the injector nozzles of the internal combustion engines with different values. So far, there has been a lack of knowledge and technical solutions regarding the methods (and a device) for measuring the friction force between the body and the needle of injector nozzles. Another advantage is the possibility of using water, which is an available, cheap and environmentally friendly medium, to enable a wide range of loadings for the friction-force measurements.

The results of the measurements are likely contribute to take the injector nozzles out of operations that are in an unfit state and to prevent their further wear by the accumulation of deposits, the limit negative impacts on the technical state of the engine, the reduction in the emission of toxic outlet components to the atmosphere from the internal combustion engine, and the reduction in frictional power losses. The values of the friction forces in the presented method can be used to calculate the fractions of the power losses in combustion engines.

The method can be used to assess the technical state of a precision pair of injector nozzles and injection pumps. The measurement of the maximum friction force applies to the nozzles before their mounting onto the injector or after disassembly. The influence of the angular position of the needle in relation to the bodies of the precision pairs in conventional combustion engines was also investigated, along with the diametral clearance between the nozzle body and needle and the surface conditions on the values of the maximum friction force. Errors in shape and position result in the uniqueness of the friction force at the mutual angular position of the needle in relation to the injector-nozzle body, and the decrease in diametral clearance and deterioration of the state of surface topography increase the friction losses.

This research has shown that many injector nozzles are approved for operation that are, in fact, in an unfit state. An unaccepted injector nozzle can be repaired and re-tested or taken out of operation.

The contributions of this work are the development of a device and a method for quantifying static and dynamic frictional forces, alongside a procedure for determining the friction losses in the injection apparatus. A model of the influence of various factors on the value of the maximum friction force in injector nozzles was also developed.

In further research, it is planned to consider the influence of thermal loads on the friction forces in the injector nozzles and friction force investigations in working internal combustion engines. It is also planned to conduct flow, material and manufacturing technique tests, leading to a reduction in friction losses.

It is important from the point of view of influencing the values of internal-combustion-engine operating parameters and minimizing frictional power losses and fuel consumption, as well as the toxicity and opacity of exhaust fumes. The construction of such equipment test stand does not require large expenditures. In reviews of the state of the knowledge and the art, it has not been found that injector nozzles are tested in this way.

7. Patents

Monieta J. Method and hydrostatic device for friction measurement. Patent of the Republic of Poland 14.01.2016 WUP 09.08.2015, No. 391224, pp. 1–6.

Funding: This research outcome has been achieved under the research project financed from a subsidy of the Ministry of Science and Higher Education for statutory activities 1/S/IESO/2014.

Data Availability Statement: Not applicable.

Acknowledgments: The author would like to thank the shipowner Polsteam for generously providing investigation samples.

Conflicts of Interest: The author declares no competing interests.

Nomenclature

a	acceleration of the injector needle	m_n	mass of the needle
E	energy stream supplied to the engine in the fuel	N	pressure force perpendicular to the surface
E_e	useful energy stream	s	the dimension of the needle nozzle perpendicular to the longitudinal axis
E_{co}	cooling losses	T_d	dynamic friction force
E_o	outlet losses	T_s	static friction force
E_{in}	energy stream of incomplete combustion losses in self-ignition engines	T_{smax}	maximum static friction force
E_h	stream of energy lost to the environment through heat exchange	T_{smaxa}	average maximum static friction force
E_o	outlet losses	N_{max}	frictional power
E_m	energy flux lost to mechanical losses	α	the angle of the inclined plane
E_r	the flux of the rest of the energy losses and the heat-balance error	$\delta(P_e)$	relative maximum error of the signal processing
c	needle-movement speed	φ	angle of position of the body and the nozzle needle
g	acceleration of gravity	$\mu_d(c)$	motion-friction coefficient
h	needle lift	μ_s	the coefficient of static friction
L_T	friction work	$\sigma(T_s)$	random absolute root means square error of the static friction force in time τ
m_a	additional mass	$\overline{\sigma}(T_s)$	random relative error of the static frictional force

References

1. Yan, R.; Wang, S.; Du, Y. Development of a two-stage ship fuel consumption prediction and reduction model for a dry bulk ship. *Transp. Res.* **2020**, *138*, 101930. [CrossRef]
2. Wong, V.W.; Tung, S.C. Overview of automotive engine friction and reduction trends-effects of surface, material, and lubricant-additive technologies. *Friction* **2016**, *4*, 1–28. [CrossRef]
3. Li, R.; Meng, X.H.; Xie, Y.B. A new coupling tribodynamic model of crosshead slipper-guide system and piston skirt-liner system of low-speed marine diesel engines. *Tribol. Int.* **2018**, *117*, 189–205. [CrossRef]
4. Delprete, C.; Gastaldi, C.; Giorio, L. A minimal input engine friction model for power loss prediction. *Lubricants* **2022**, *10*, 94. [CrossRef]
5. Monieta, J. Selection of diagnostic symptoms and injection subsystems of marine reciprocating internal combustion engines. *Appl. Sci.* **2019**, *9*, 1540. [CrossRef]
6. Monieta, J. Research on the friction force of the needle in the nozzle body of marine diesel engines in the presence of a lubricating medium that account position changes. *Tribologia* **2012**, *2*, 41–57.
7. Monieta, J.; Lorek, Ł. Researches of friction force of injector nozzles in injector bodies of marine diesel engines in the presence of lubricating compound. *J. Pol. CIMAC* **2008**, *3*, 111–121.
8. Monieta, J.; Kasyk, L. Optimization of design and technology of injector nozzles in terms of minimizing energy losses on friction in compression ignition engines. *Appl. Sci.* **2021**, *11*, 7341. [CrossRef]
9. Bielawski, P. Diagnosing machines with the use of friction. *Diagnostics* **2003**, *29*, 15–20.

10. Fadel, C.; Chalhoub, N.G.; Kfoury, G.A. Direct measurement of the piston-assembly friction force in a single cylinder engine under motoring conditions. In Proceedings of the 1st Annual Dynamic Systems and Control Conference 2008, Ann Arbor, MI, USA, 20–22 October 2008; pp. 20–22. [CrossRef]
11. Karczewski, M.; Szczęch, L. Investigation of internal resistance of a diesel engine. *Sci. J. PNA* **2013**, *193*, 27–49.
12. Aydin, Z.; Savas, Ö.; Parlak, A.; Keskin, I.; Ünlügençoglu, K. Effects of fuel contamination to marine lubricant. *Acta Phys. Pol.* **2016**, *129*, 1–4. [CrossRef]
13. Truhan, J.J.; Qu, J.; Blau, P.J. The effect of lubricating oil condition on the friction and wear of piston ring and cylinder liner materials in a reciprocating bench test. *Wear* **2005**, *259*, 1048–1055. [CrossRef]
14. Ruddy, B.L.; Dowson, D.; Economus, P.N. A theoretical analysis of the twin land type of oil-control piston ring. *J. Mech. Eng. Sci.* **1981**, *23*, 51–62. [CrossRef]
15. Livanos, G.A.; Kyrtatos, N.P. Friction model of a marine diesel engine piston assembly. *Tribol. Int.* **2007**, *40*, 1441–1453. [CrossRef]
16. Vølund, A. Measurement and Calculation of Frictional Loss in Large Two-Stroke Engines. Ph.D. Thesis, Technical University of Denmark, Lyngby, Denmark, 2003; pp. 1–200.
17. Knauder, C.; Allmaier, H.; Sander, D.E.; Sams, T. Investigations of the friction losses of different engine concepts. *Lubricants* **2019**, *7*, 39. [CrossRef]
18. Wang, Z.J.; Shuai, S.J.; Li, Z.J.; Yu, W.B. A Review of Energy Loss Reduction Technologies for Internal Combustion Engines to Improve Brake Thermal Efficiency. *Energies* **2021**, *14*, 6656. [CrossRef]
19. Abril, S.O.; Rojas, J.P.; Florez, E.N. Numerical methodology for determining the energy losses in auxiliary systems and friction processes applied to low displacement diesel engines. *Lubricants* **2020**, *8*, 103. [CrossRef]
20. Idzior, M. A Study of Combustion Ignition Engine Injector Nozzle Parameters in the Aspect of Operating Properties. Scientific Dissertations, Poznan University of Technology, Poznan, Poland, 2004; pp. 51–139.
21. Stöeckli, M.; Affolter, P.; Otto, H. Durability and long-term stability of electronic fuel injection systems for Diesel, HFO and gas engines. In Proceedings of the 25th CIMAC Congress 2007, Viena, Austria, 21–24 May 2007; pp. 1–9.
22. Włodarski, J.K. *Reciprocating Internal Combustion Engines—Tribological Processes*; Publishing House of Communication and Communications: Warsaw, Poland, 1982; pp. 56–63.
23. Baratta, M.; Catania, A.E.; Pesce, F.C. CNG Injector Nozzle Design and Flow Prediction. In Proceedings of the ASME 2010 Internal Combustion Engine Division Fall Technical Conference, San Antonio, TX, USA, 12–15 September 2010; pp. 795–800. [CrossRef]
24. Włodarski, J.K. *Operating States of Marine Combustion Engines*; Maritime University of Gdynia Publisher: Gdynia, Poland, 2001; pp. 159–178.
25. Hebda, M. *Friction, Lubrication and Wear Processes of Machines*; Publisher of the Institute of Sustainable Technologies: Warsaw, Poland; Radom, Poland, 2007; pp. 155–455.
26. Drozdowski, J. *A Study on Thermal Loads, Cavitation and Reliability of Marine Diesel Engine Fuel Injectors. Study 30*; Maritime University Szczecin: Szczecin, Poland, 1998; pp. 33–84.
27. Daimler, C.; Güttler, J.; Hora, P. Einspritzdüse für in Einspritzsystem sowie ein Erfahren zur Herstellung einer Einspritzdüse eines Einspritzsystem eines Kraftfahrzeuges. Deutschland Patent 10256590, 3 June 2004.
28. Monieta, J.; Łukomski, M. Methods and means of estimation of technical state features of the marine diesel engines injector nozzles type Sulzer 6AL20/24. *Sci. J. Marit. Univ. Szczec.* **2005**, *5*, 383–392.
29. Theodorakakos, A.; Strotos, G.; Mitroglou, N.; Atkin, C.; Gavaises, M. Friction-induced heating in nozzle hole micro-channels under extreme fuel pressurisation. *Fuel* **2014**, *123*, 143–150. [CrossRef]
30. Strotos, G.; Koukouvinis, P.; Theodorakakos, A.; Gavaises, M.; Bergeles, G. Transient heating effects in high pressure Diesel injector nozzles. *Int. J. Heat Fluid Flow* **2015**, *51*, 257–267. [CrossRef]
31. Vidal, A.; Kolovos, K.; Gold, M.R.; Pearson, R.; Koukouvinis, P.; Gavaises, M. Preferential cavitation and friction-induced heating of multi-component Diesel fuel surrogates up to 450 MPa. *Int. J. Heat Mass Transf.* **2021**, *166*, 120744. [CrossRef]
32. Szczerek, M.; Tuszyński, W. *Tribological Studies. Seizure*; ITeE: Radom, Poland, 2000; pp. 7–142.
33. Yasunori, K. Fuel Injection Nozzle. U.S. Patent 20020109021A1, 15 August 2002.
34. Yasunori, K.; Takashi, I. Fuel Injection Nozzle with a Member to Reduce the Frictional Force Developed between Parts during the Clamping. EP Patent 1236887A3, 14 January 2004.
35. Holmberg, K.; Andersson, P.; Nylund, N.O.; Mäkelä, K.; Erdemir, A. Global energy consumption due to friction in trucks and buses. *Tribol. Int.* **2014**, *78*, 94–114. [CrossRef]
36. Zabelin, P. Internal Combustion Engine Efficiency. U.S. Patent 20140318507A1, 30 October 2014.
37. Longwic, R.; Sander, P.; Górski, K.; Jańczuk, B.; Zdziennicka, A.; Szymczyk, K. The new concept of using rapeseed oil as a fuel to power diesel engines. *Rail Transp. Tech.* **2013**, *10*, 2877–2899.
38. Lopez, J.J.; Salvador, F.J.; de la Garza, O.A. Characterization of the pressure losses in a common rail diesel injector. *Proc. Inst. Mech. Eng.* **2012**, *226*, 1697–1706. [CrossRef]
39. Ciornei, F.C.; Alaci, S.; Romanu, I.C.; Mihai, I.; Lazar, V.C. Aspects concerning the friction for the motion on an inclined plane of an axisymmetric body. *Mater. Sci. Eng.* **2019**, *477*, 1–10. [CrossRef]
40. Dudziak, M.; Domek, G.; Kołodziej, A.; Talaśka, K. Contact problems between the hub and the shaft with a three-angular shape of cross-section for different angular positions. *Procedia Eng.* **2014**, *96*, 50–58. [CrossRef]
41. Piaseczny, L. *Repair Technology of Marine Internal Combustion Engines*; Maritime Publisher: Gdansk, Poland, 1992; pp. 352–414.

42. Farth, A.; Volgt, A.; Spickenreuther, M. Method for Setting the Nozzle Opening Pressure for an Injection Nozzle and Arrangement for Carrying out the Method. U.S. Patent 6976389 B2, 13 June 2002.
43. Vinogradov, M.; Dorfman, V. Method and Device for Measuring Forces. U.S. Patent WO2003036249A1, 1 May 2003.
44. Kelemenova, T.; Dovica, M.; Bozek, P.; Koláriková, I.; Benedik, O.; Virgala, I.; Prada, E.; Mikova, L.; Kot, L.; Kelemen, M. Specific problems in measurement of coefficient of friction using variable incidence tribometer. *Symmetry* **2020**, *12*, 1235. [CrossRef]